

Experimental and theoretical evidence for a hydrogen stabilized $c(2 \times 2)$ reconstruction of the P-rich InP(001) surface

T. Letzig* and F. Willig†

Hahn-Meitner-Institut, SE4 Dynamics of Interfacial Reactions, Glienicke Straße 100, 14109 Berlin, Germany

P. H. Hahn

Institut für Festkörpertheorie und -optik, Friedrich-Schiller-Universität, Max-Wien-Platz 1, 07743 Jena, Germany

W. G. Schmidt‡

Theoretische Physik, Universität Paderborn, 33095 Paderborn, Germany

(Received 3 August 2006; revised manuscript received 7 September 2006; published 8 December 2006)

The formation of hydrogen bonds was investigated on the P-rich InP(001) surface employing attenuated total-reflection Fourier-transform infrared spectroscopy, low-energy electron diffraction, and total-energy density-functional theory calculations. Strong evidence was found for a $c(2 \times 2)$ -2P-3H reconstruction with a higher hydrogen coverage than is characteristic for the metal-organic chemical-vapor deposition prepared hydrogen-stabilized (2×2) -2D-2H surface. The new surface reconstruction was formed upon exposure to atomic hydrogen. Complete transformation of all the metastable atomic configurations to form the new surface reconstruction was not achieved, since prior to this the surface began to deteriorate. The latter effect was monitored as the formation of In-H bonds. Two observations, i.e., nearly complete screening of the infrared peaks for excitation with p -polarized light and a pronounced redshift of P-H peaks with increasing hydrogen coverage were attributed to dipole-dipole interaction between the vibrating adsorbates.

DOI: [10.1103/PhysRevB.74.245307](https://doi.org/10.1103/PhysRevB.74.245307)

PACS number(s): 68.35.Bs, 68.43.Bc, 68.43.Pq, 78.55.Cr

I. INTRODUCTION

The III-V(001) surfaces are model cases for exploring the driving forces for semiconductor surface reconstructions.^{1,2} In this context, the InP(001) $p(2 \times 2)/c(4 \times 2)$ surface³ has found particular attention, because this surface reconstruction does not obey the so-called electron-counting rule. This rule (see, e.g., Ref. 4) postulates uncharged and semiconducting surfaces with empty cation dangling bonds and filled anion dangling bonds. It has been found to govern the vast majority of compound semiconductor surfaces. III-V(001) surface reconstructions smaller than (4×2) necessarily violate the electron-counting principle. In order to explain the observation of a semiconducting $p(2 \times 2)$ reconstruction on MOCVD-grown InP(001) surfaces, the manifestation of many-body effects, namely, strong electron correlation across the P-dimer rows was suggested.³ Later it was shown that, in fact, hydrogen stabilizes the $p(2 \times 2)$ surface.⁵⁻⁸ In the present study we revisit the InP(001) surface using low-energy electron diffraction (LEED) and infrared (IR) spectroscopy and find evidence for a $c(2 \times 2)$ surface reconstruction with more hydrogen in the unit cell compared to the $p(2 \times 2)$ geometry described in Refs. 3 and 5. The introduction of additional P-H bonds into the new unit cell was achieved here only by exposure to atomic hydrogen outside the MOCVD reactor. Based on first-principles density-functional theory (DFT) calculations, a structural model is proposed with three hydrogen atoms in the $c(2 \times 2)$ unit cell of P-terminated InP(001).

II. METHODOLOGY

A. Experiment

Layers of indium phosphide (InP) of about 200 nm thickness were grown on an InP(001) wafer in an AIX 200 reactor

via MOCVD. The substrate was a semi-insulating InP wafer from InPact, 530- μm -thick, and cut with an uncertainty of 0.2° with respect to the exact (001) surface. Prior to growing the layer the wafer was cut to a parallelepipedal shape with a base angle of 45° . This allowed for multipass Fourier transform infrared (FTIR) measurements of the P-H bonds formed on the surface making use of ATR (attenuated total reflection). The layer was grown with tertiarybutylphosphine (TBP) and trimethylindium (TMI) as precursors at a V/III ratio of 20 and partial pressures of 3.2×10^{-1} mbar and 1.6×10^{-2} mbar, respectively.⁹ Hydrogen served as the carrier gas at a pressure of 100 mbar. The P-rich surface of InP(001) was prepared according to the procedure described in Refs. 8 and 10. After preparing the surface the sample was transferred to different UHV (ultrahigh vacuum) analysis chambers utilizing an MOCVD-UHV transfer system and a mobile UHV chamber with sample transfer via load-lock ports.¹¹ The as-grown sample surface was investigated without applying any further post-transfer surface preparation. We have shown before⁸ that the as-grown surface is characterized by IR peaks that agree with the postulated two P-H bonds per surface unit cell.⁶ LEED measurements were performed using LEED optics from Specs. Infrared spectra were recorded with a Bruker IFS66v spectrometer combined with an UHV chamber. The complete experimental setup is described elsewhere.¹² As usual for ATR spectra the intensity of vibrational absorption bands is given here in units of change in reflectance normalized to the number of reflections inside the ATR crystal. IR peaks were obtained from difference measurements following the procedure described in detail in Ref. 8. The hydrogen pressure in the UHV chamber was measured with a cold cathode (Pfeiffer, IKR270). Throughout this work the hydrogen exposure is given in Langmuir

units using the pressure measured with this cold cathode calibrated to molecular hydrogen. Switching on a filament placed about 2 cm in front of the sample led to a percentage on the order of 0.05 atomic hydrogen. It is important to note that already the cold-cathode-contributed atomic hydrogen at about a factor of 10^3 lower rate than the hot filament. If not stated otherwise this gentle source of atomic hydrogen is used in the experiments. It is shown later that only atomic hydrogen was effective in changing the surface reconstruction.

B. Theory

Total-energy calculations were based on a massively parallel, real-space finite-difference implementation¹³ of the density-functional theory in the local-density approximation (DFT-LDA). A multigrid technique was employed for convergence acceleration. The computational details were equal to those of Ref. 5, in order to allow for a meaningful comparison. Due to the varying surface stoichiometry, the thermodynamic grand-canonical potential Ω in dependence upon the chemical potentials μ of the surface constituents needs to be calculated in order to determine the surface ground state. The In and P chemical potentials cannot vary independently because the surface is in equilibrium with bulk InP. Correspondingly, it holds $\mu(\text{In}) + \mu(\text{P}) = \mu(\text{InP})_{\text{bulk}}$, and the surface phase diagram may be shown in dependence on only two variables, which we take as the chemical potentials of In and H. Here $\Delta\mu(\text{H})=0$ corresponds to the situation where the surface is exposed to molecular hydrogen at $T=0$. Increasing the temperature lowers the hydrogen chemical potential, whereas exposure to atomic hydrogen leads to an increase in $\Delta\mu(\text{H})$. The temperature and pressure dependence of $\Delta\mu(\text{H})$ can be approximated by that of a diatomic ideal gas. The respective temperature and pressure dependence has been shown in Fig. 3 in Ref. 6.

III. RESULTS AND DISCUSSION

The MOCVD-prepared P-rich $p(2 \times 2)/c(4 \times 2)$ surface [sometimes addressed as (2×1) based on the apparent LEED pattern (see Fig. 1, left-hand side)] has been labeled (2×2) -2D-2H.⁶ 2D and 2H stand for two P dimers and two hydrogen atoms in the topmost layer of the unit cell, respectively. To check whether a stable phase with more hydrogen bonds can be prepared by exposing the (2×2) -2D-2H surface to a higher pressure of molecular hydrogen, this surface was first exposed in the MOCVD reactor at room temperature up to the highest pressure that could be realized, i.e., about 900 mbar molecular hydrogen. No significant change of the surface could be detected, however, using reflection anisotropy spectroscopy (RAS) and infrared spectroscopy. Since the activation energy is unknown the above result does not disprove the possibility of a phase transition to a stable reconstruction with more hydrogen bonds. Exposure to atomic hydrogen was realized after sample transfer to the UHV chamber where the sample could be addressed with FTIR measurements. After exposure of the (2×2) -2D-2H surface to atomic hydrogen a LEED pattern was observed

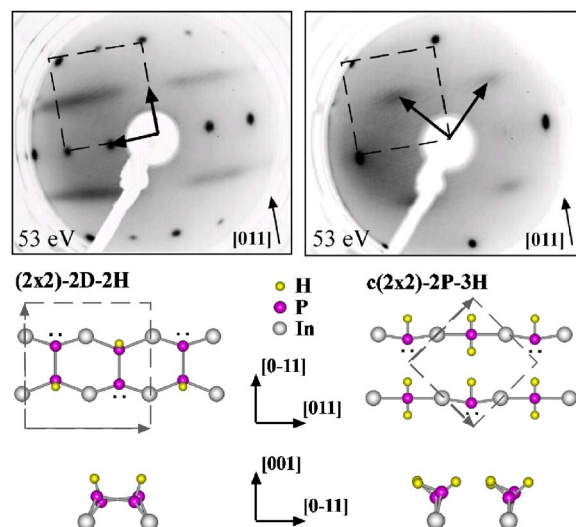


FIG. 1. (Color online) Inverted LEED images of the (2×2) -2D-2H (left-hand side) and $c(2 \times 2)$ -2P-3H (right-hand side) surface reconstructions. Top and side views of the corresponding surface reconstructions with unit cells marked at the bottom as dashed squares. The positions of the atoms are according to the calculations. Two black dots represent a filled dangling bond. The other dashed squares drawn in the LEED images indicate the size of a (1×1) surface unit cell. The arrows indicate the reciprocal lattice vectors and the primitive translations, respectively.

that is shown at the right-hand side of Fig. 1 at the top. The half-order spots appear somewhat diffuse, nevertheless, a (centered) $c(2 \times 2)$ reconstruction can be clearly identified. From intuition it was clear looking at the (2×2) -2D-2H that there is the possibility of surface reconstructions with a higher percentage of P-H bonds where the electron counting rule is obeyed. The atomic arrangement in the plausible $c(2 \times 2)$ -2P-3H unit cell (see Fig. 1 right-hand side, bottom) would agree with the $c(2 \times 2)$ LEED pattern. This $c(2 \times 2)$ unit cell is the only centered one which fulfills the electron-counting rule. It is thus postulated here as a new surface reconstruction of InP(001). In some cases the new LEED image explained above appeared more as a (2×1) reconstruction (not shown here) but this phenomenon is already well known from the (2×2) -2D-2H reconstructed surface, where two differently reconstructed domains exist on the surface.^{3,8} In the case of the $c(2 \times 2)$ -2P-3H reconstruction every second row must be shifted by $a/\sqrt{2}$ (if a represents the bulk lattice constant) in the $[0\bar{1}1]$ direction whereby a (2×1) reconstruction is obtained. There are of course other related reconstructions conceivable and this point will be addressed below. The LEED pattern and the geometry of the (2×2) -2D-2H reconstructed surface with which the preparation had started is shown for comparison at the left-hand side of Fig. 1. The polarized infrared spectra due to P-H stretching vibrations are shown in Fig. 2 and for the same surface whose LEED image can be seen in Fig. 1, right-hand side. The negative peak for the B_0 mode stems from the MOCVD prepared (2×2) -2D-2H surface⁸ that was used as the reference for obtaining the difference spectra shown in Fig. 2. There is a frequency splitting between the symmetric

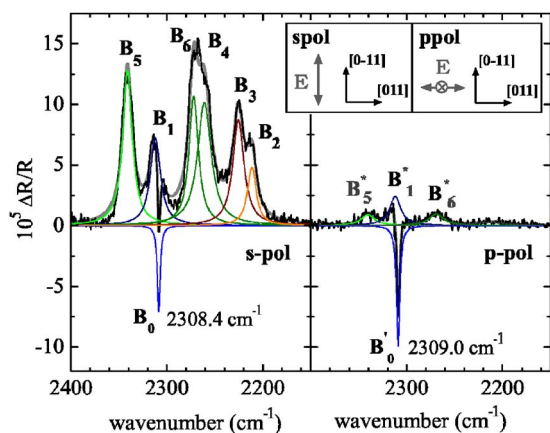


FIG. 2. (Color online) FTIR-ATR polarization-dependent spectra of the P-H stretching vibrations after the MOCVD-prepared P-rich (2×2) -2D-2H InP(001) surface was exposed to about $350 \times 10^4 L$ H_2 . Lorentzian fits to all the separate peaks are shown. The spectral resolution was 1 cm^{-1} . The inset shows the directions of the electric-field vectors relative to the crystal orientation (compare with Fig. 1).

and the antisymmetric vibration of the two P-H bonds in the latter unit cell (see Fig. 1, left-hand side, bottom) that was measured here as 0.6 cm^{-1} . The negative intensity of the B_0 mode in the difference spectra and the appearance of several positive P-H modes indicate unambiguously that the surface reconstruction was changing upon exposure to atomic hydrogen. The above-postulated $c(2 \times 2)$ -2P-3H reconstruction should give rise to two P-H modes for s -polarized light, i.e., first the antisymmetric mode from the dihydride and second the mode from the monohydride. Obviously, the spectrum in Fig. 2 does not show two but six modes (positive peaks, where the negative peak is due to the reference in the difference spectrum) that are labeled B_1 to B_6 . All the six modes can be clearly resolved by a fit with a Lorentzian line shape, and the corresponding frequencies are listed in Table I. The FWHM of B_0 is 4 cm^{-1} whereas the FWHM of the other modes varies between 8 and 19 cm^{-1} . We consider the fact that no In-H peaks have developed when peaks B_1 – B_6 are rising as proof for a still undestroyed surface. Considering the frequencies for possible metastable atomic configurations and for the two stable modes in the $c(2 \times 2)$ -2P-3H unit cell we assign peak B_3 (monohydride) and peak B_5 (dihydride) to the modes of the complete $c(2 \times 2)$ -2P-3H reconstruction. This hypothesis finds some support in the observation that these two peaks are decreasing only after some of the other peaks shown in Fig. 2 have already started to decrease at lower hydrogen supply. The assignment of the two peaks is also supported by a cluster calculation published earlier by

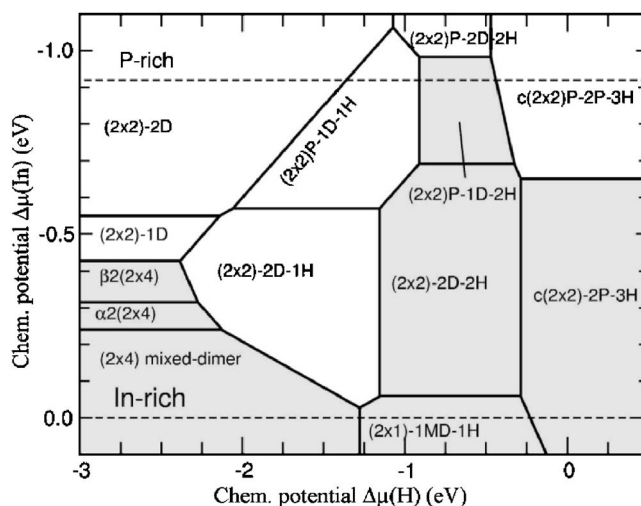


FIG. 3. Calculated InP(001) surface-phase diagram including the $c(2 \times 2)$ -2P-3H reconstruction. Gray-shaded reconstructions fulfill the electron-counting rule.

the Hicks group.¹⁴ We attribute three positive peaks to metastable transition states (atomic structures) that are being formed upon exposure to atomic hydrogen. In the absence of further side reactions the latter peaks should disappear upon further exposure to atomic hydrogen with only the two expected positive peaks remaining. Before discussing in some more detail all the peaks seen in Fig. 2 we would like to present strong theoretical support for the above hypothesis of a new InP(001) hydrogen-bonded surface reconstruction.

We investigated here a series of conceivable surface structures with first-principle calculations in addition to the geometries studied earlier.⁶ Only two of them a (2×1) and the above $c(2 \times 2)$ reconstruction are compatible with the observed LEED pattern. Moreover, the $c(2 \times 2)$ -2P-3H reconstruction turned out very robust, similar to the (2×2) -2D-2H with lower P-H content, with the energy of all other conceivable structures removed by at least 0.05 eV to higher energies. By choosing equivalent k -point sets and keeping the numerical parameters constant for all surface structures considered, we estimate the error for the relative surface energies below 50 meV. Over a wide range of the In chemical potential the calculations predict for InP surfaces exposed to a high concentration of hydrogen, the structure that we called $c(2 \times 2)$ -2P-3H (Fig. 1, bottom right; see the calculated phase diagram in Fig. 3). This surface reconstruction obeys the electron-counting rule and can explain at least part of the experimental findings.

The complete transition from phase (2×2) -2D-2H to phase $c(2 \times 2)$ -2P-3H was unfortunately not achieved by supplying atomic hydrogen. It will be shown below that the

TABLE I. Mean frequencies of the P-H stretching vibrations measured with unpolarized light and frequency shift depending on hydrogen coverage.

	B_5	B_1	B_0	B_6	B_4	B_3	B_2
$\bar{\nu} \text{ (cm}^{-1}\text{)}$	2340	2312	2308.9	2265	2256	2232	2215
$\pm \Delta \bar{\nu} \text{ (cm}^{-1}\text{)}$	4	1	0.3	5	4	8	3

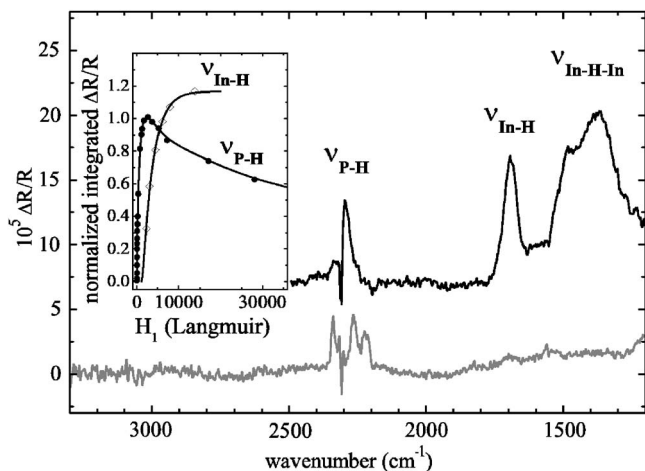


FIG. 4. Infrared spectra of the P-rich prepared surface after exposure to some 100L (gray curve) and some 10 000L (black curve, shifted for clarity) of hydrogen. Atomic hydrogen was produced here with the hot tungsten filament mounted in front of the sample. The spectral resolution was 4 cm^{-1} . The inset shows the integrated intensity of the P-H and In-H stretching modes, respectively, versus exposure to hydrogen.

surface started to deteriorate with the formation of In-H bonds before the peaks B_2 , B_4 , and B_6 , assigned to metastable atomic configurations, had disappeared. The activation energies to be surmounted for further attachment of hydrogen to any of the atomic configuration that appear plausible for the metastable transition states are not known. Finding the activation energies would have required detailed temperature-dependent measurements for which our UHV chamber was not equipped. It is, however, obvious that the activation energies for destroying the P-rich crystal surface, which can be recognized by the appearance of In-H peaks (Fig. 4), must be of similar magnitude as those required for the further attachment of hydrogen to the metastable atomic configurations. Otherwise the $c(2 \times 2)$ -2P-3H phase would have been established everywhere on the surface before the surface started to deteriorate.

We discuss in the following, in more detail, plausible atomic configurations for the metastable transition states and the behavior of the IR peaks when the surface is exposed for a longer time to atomic hydrogen, i.e., we discuss the attachment of further hydrogen at the surface and its deterioration seen in the formation of In-H bonds when both processes are occurring in later stages in parallel (Fig. 4). It is proposed here that the vibrational frequency B_1 stems from the (2×2) -2D-2H unit cell, where one hydrogen atom is bonded to a P dimer but where the neighboring P atoms are now already bonded to more than one hydrogen atom. The frequency of the B_1 peak is very close to that of the B_0 peak and shows virtually the same rate for its formation as the peak B_0 shows for its decrease with ongoing exposure to atomic hydrogen. Peaks B_2 , B_4 , and B_6 are suggested to belong to metastable atomic configurations. Our suggestion agrees with the earlier proposal by the Hicks group that peaks B_4 and B_6 are the modes of two hydrogen atoms bonded to an intact P dimer.¹⁴ It is, however, ruled out here that the peaks

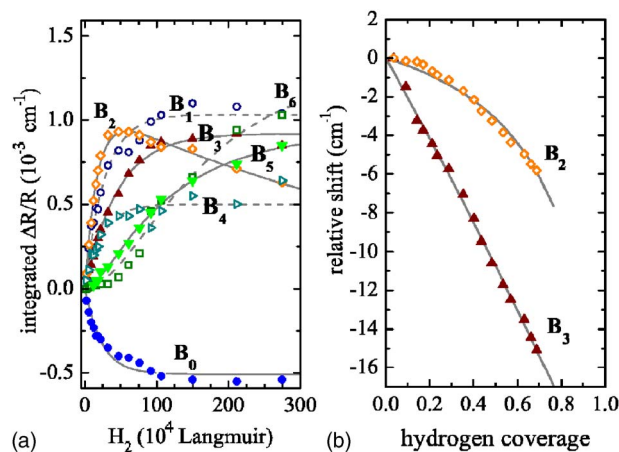


FIG. 5. (Color online) (a) Integrated intensities of the P-H vibrations (compare with Fig. 2) vs hydrogen exposure. Fit curves (first-order Langmuir isotherms) are given as a guide to the eye. (b) Frequency shifts of two P-H modes versus normalized hydrogen coverage.

correspond to the antisymmetric and the corresponding symmetric mode since both modes showed strong intensities in the spectrum measured with *s*-polarized light (Fig. 2, left-hand side). A more plausible suggestion for the origin of these peaks appears to be two antisymmetric modes of two hydrogen atoms bonded to an intact P dimer but the latter exposed to different atomic environments, e.g., where in one case the adjacent P dimer has already fissured and in the other case it has not. B_2 has to be a metastable state since its intensity is decreasing very early upon further exposure to atomic hydrogen. This can be seen in Fig. 5(a) showing the integrated intensity of every P-H mode versus hydrogen exposure. The frequency of B_2 is close to that of B_3 and is therefore tentatively assigned to a hydrogen atom bonded to a P atom with a dangling bond filled with only one electron instead of two as is assumed in the case of the peak B_3 . A half-filled dangling bond should not be very stable and may explain the early decrease of B_2 . A difficulty arises for these assignments from the fact that no strong positive modes were detected with *p*-polarized light (Fig. 2, right-hand side). This prevented the identification of antisymmetric vibrations with corresponding peaks of the symmetric vibrations. The most plausible reason for the at first very surprising low intensity measured with *p*-polarized light is given below. In addition to polarization-dependent measurements isotopic-mixture experiments are in general helpful in making band assignments. Such experiments were performed also for the present system. There were indeed weak shoulders among the P-H peaks due to vibrations of mixed dihydrides (H-P-D; D = deuterium), but unfortunately they could not be unambiguously assigned to the respective peaks. Moreover, the spectral separation of all the P-D peaks was not achieved due to the smaller distances between these peaks (heavier mass of the D atoms) and the larger noise of the detector that had to be used in that spectral range. Metastable states are expected to disappear when the stable reconstruction is established everywhere at the surface and the hydrogen bonds of the respective reconstruction have reached the saturation cover-

age. Unfortunately, some of the peaks attributed to metastable atomic configurations, i.e., B₄ and B₆, remain until the surface shows already signs of deterioration. The deterioration or etching of the InP(001) surface upon exposure to a greater amount of atomic hydrogen is already established in the literature.¹⁵ A corresponding IR spectrum is shown in Fig. 4 for a P-rich prepared surface after exposure to an oversupply of atomic hydrogen (black curve). Vibrations have appeared that should not occur at an ordered P-rich surface, most notably peaks of In-H vibrations (between 1800 and 1200 cm⁻¹).¹⁶ Peaks B₁–B₆ have vanished now and the rather broad P-H band appearing around 2300 cm⁻¹ is tentatively attributed here to –PH₃ species. Silicon surfaces terminated with –PH₃ exhibit vibrational bands around this frequency.¹⁷ It is important to add here that the infrared spectrum of an originally In-rich prepared InP(001) surface looks at the end of an oversupply of atomic hydrogen (not shown here) rather similar to the upper spectrum shown in Fig. 4. Further investigations appear necessary to probe whether preparation procedures can be found for the c(2 × 2)-2P-3H reconstruction that can avoid the simultaneous destruction of the P-rich surface. The additional supply of phosphorus together with atomic hydrogen could be attempted in future work. Another alternative could be the use of a pressure cell where a high pressure of molecular hydrogen can be applied.

The at first surprising observation shown in Fig. 2 at the right-hand side will now be discussed. It is well known that the intensity of vibrational modes can be screened and frequencies can be shifted with increasing coverage of the adsorbates.^{18,19} Sometimes a macroscopic model, the so-called three-layer model,^{20,21} has been used to describe this screening effect. The obvious shortcoming of the latter approach is that no downshift in vibrational frequencies can be modeled within the three-layer models available in the literature. There is the more satisfying microscopic theory for the dipole-dipole interaction between vibrating adsorbates^{18,22–26} where the screening effect and the shift are related to the polarizability of the adsorbate complex. In the simplest case of only one perpendicular ($j = \perp$) or only one parallel ($j = \parallel$) mode the screening in intensity I_j for a complete adsorbate layer is given by

$$I_j \propto \frac{1}{\left(1 + \frac{1}{4\pi\epsilon_0} \alpha_{e,j} U_{0,j}\right)^2}, \quad (1)$$

and the relative frequency shift in dependence on coverage Θ is given by

$$\Delta\bar{\nu} = \bar{\nu}_0 \left(\sqrt{1 + \frac{\frac{1}{4\pi\epsilon_0} \alpha_{v,j} \Theta U_{0,j}}{\left(1 + \frac{1}{4\pi\epsilon_0} \alpha_{e,j} \Theta U_{0,j}\right)}} - 1 \right), \quad (2)$$

where α_v and α_e are the vibrational and electronic part of the polarizability, respectively, $U_{0,j}$ is a surface-lattice sum, and

ϵ_0 is the permittivity of vacuum. $\bar{\nu}_0$ is the vibrational frequency near-zero coverage. Both equations are given here in SI units. For a square lattice the relations always hold that $U_{0,\perp} > 0$ and $U_{0,\parallel} = -0.5/U_{0,\perp} < 0$. Making use of Eqs. (1) and (2) and the latter inequalities one can explain, e.g., the screening of the intensity for perpendicular modes and the downshift in frequency for parallel modes. In the case of the H-terminated P-rich InP(001) surface investigated in this work the screening seems to be larger than has been found on the H-terminated silicon surface. Since the H-coverage appears comparable, the reason for this difference must be sought in a higher electronic polarizability of the P-H compared to the Si-H adsorbate complex. Only a few publications report on a downshift (or redshift) of vibrational frequencies with increasing adsorbate coverage (see, e.g., Refs. 27–29). Most of the investigations of adsorbates have been carried out for metallic surfaces. The surface-selection rule on metals (the electric field parallel to the surface is screened completely) prohibit in most cases the detection of parallel vibrational modes. Figure 5(b) shows the downshifts of two P-H modes on InP(001) that we measured in a reproducible way. Lacking a method for measuring the absolute hydrogen coverage, we plotted in Fig. 5(b) an approximate coverage that was calculated as the integral over the intensity of all the P-H vibrations at a given hydrogen exposure, and this signal was normalized against the value at the maximum of the curve labeled ν_{PH} in the inset of Fig. 4. The gray curves in Fig. 5(b) are fits with Eq. (2). In a simple case two characteristic values of the adsorbate complex, i.e., α_v and α_e , can be determined from the fit. In the present system there are unfortunately many unknown parameters, and thus these values cannot be determined with any reliable accuracy. Complicating factors are here: additional chemical shifts that are independent of coverage^{19,30} (in principle, the latter could be addressed with isotopic-mixture experiments), the interaction between many different vibrational modes,²⁴ the unknown single-mode coverage, the bond angle for uncoupled modes,¹² the image-dipole contribution to the lattice sum,^{12,28} and perhaps a multipole contribution beyond the dipole-dipole approximation.³¹ Surprisingly, to our knowledge the better-defined hydrogen-terminated silicon surfaces have not yet been addressed with the microscopic dipole-dipole interaction theory.

IV. CONCLUSIONS

The MOCVD-prepared P-rich surface of InP(001) was exposed to atomic hydrogen. LEED images and infrared spectra recorded after this exposure give evidence for a change towards a reconstruction with more H atoms per unit cell compared to the MOCVD-prepared surface. DFT calculations predict a stable c(2 × 2) reconstruction with three H atoms per unit cell. Unfortunately, the surface started to deteriorate before the ideal-ordered surface with the higher hydrogen content was reached upon exposure to atomic hydrogen. Intensity screening and frequency shifts of adsorbate vibrations observed here on the InP surface are interpreted in terms of dipole-dipole interaction.

ACKNOWLEDGMENTS

T.L. thanks the German Science Foundation (SPP 1093) for financial support. Generous grants of computer time from the Höchstleistungsrechenzentrum Stuttgart (HLRS) and the Paderborn Center for Parallel Computing are gratefully ac-

knowledged. It is a pleasure to thank B. N. J. Persson for valuable discussions concerning the dipole-dipole interaction, T. Hannappel for substantial help in planning and building the UHV-FTIR setup, and Z. Kollonitsch for assistance with the MOCVD preparation of the samples.

*Electronic address: letzig@hmi.de

†Electronic address: willig@hmi.de

‡Electronic address: w.g.schmidt@upb.de

¹W. Mönch, *Semiconductor Surfaces and Interfaces* (Springer-Verlag, Berlin, 2001).

²W. G. Schmidt, *Appl. Phys. A: Mater. Sci. Process.* **75**, 89 (2002).

³L. Li, B.-K. Han, Q. Fu, and R. F. Hicks, *Phys. Rev. Lett.* **82**, 1879 (1999).

⁴M. D. Pashley, *Phys. Rev. B* **40**, 10481 (1989).

⁵W. G. Schmidt, P. H. Hahn, F. Bechstedt, N. Esser, P. Vogt, A. Wange, and W. Richter, *Phys. Rev. Lett.* **90**, 126101 (2003).

⁶P. H. Hahn and W. G. Schmidt, *Surf. Rev. Lett.* **10**, 163 (2003).

⁷G. Chen, S. F. Cheng, D. J. Tobin, L. Li, K. Raghavachari, and R. F. Hicks, *Phys. Rev. B* **68**, 121303(R) (2003).

⁸T. Letzig, H.-J. Schimper, T. Hannappel, and F. Willig, *Phys. Rev. B* **71**, 033308 (2005).

⁹The same precursor partial pressures were used in Ref. 8 as in this work, Erratum to *Phys. Rev. B* **71**, 033308 (2005) (to be published).

¹⁰T. Hannappel, L. Töben, S. Visbeck, H.-J. Crawack, C. Pettenkofer, and F. Willig, *Surf. Sci. Lett.* **470**, L1 (2000).

¹¹T. Hannappel, S. Visbeck, L. Töben, and F. Willig, *Rev. Sci. Instrum.* **75**, 1297 (2004).

¹²T. Letzig, Ph.D. thesis, Ruhr-Universität Bochum, Germany, 2005.

¹³E. L. Briggs, D. J. Sullivan, and J. Bernholc, *Phys. Rev. B* **54**, 14362 (1996).

¹⁴Q. Fu, E. Negro, G. Chen, D. C. Law, C. H. Li, R. F. Hicks, and K. Raghavachari, *Phys. Rev. B* **65**, 075318 (2002).

¹⁵F. Stietz, T. Allinger, V. Polyakov, J. Woll, A. Goldmann, W.

Erfurth, G. Lapeyre, and J. Schaefer, *Appl. Surf. Sci.* **104/105**, 169 (1996).

¹⁶K. Raghavachari, Q. Fu, G. Chen, L. Li, C. H. Li, D. C. Law, and R. F. Hicks, *J. Am. Chem. Soc.* **124**, 15119 (2002).

¹⁷J. Shan, Y. Wang, and R. J. Hamers, *J. Phys. Chem.* **100**, 4961 (1996).

¹⁸G. Mahan and A. Lucas, *J. Chem. Phys.* **68**, 1344 (1978).

¹⁹Y. Chabal, *Surf. Sci. Rep.* **8**, 211 (1988).

²⁰J. McIntyre and D. Aspnes, *Surf. Sci.* **24**, 417 (1971).

²¹Y. J. Chabal, in *Vibrational Properties at Semiconductor Surfaces and Interfaces*, *Semiconductor Interfaces: Formation and Properties*, Vol. 22 (Springer, New York, 1987).

²²R. M. Hammaker, S. A. Francis, and R. P. Eischens, *Spectrochim. Acta* **21**, 1295 (1965).

²³M. Scheffler, *Surf. Sci.* **81**, 562 (1979).

²⁴B. N. J. Persson and R. Ryberg, *Phys. Rev. B* **24**, 6954 (1981).

²⁵R. F. Willis, A. A. Lucas, and G. D. Mahan, in *Vibrational Properties of Adsorbed Molecules*, *The Chemical Physics of Solid Surfaces and Heterogeneous Catalysis*, Vol. 2 (Elsevier, New York, 1983).

²⁶B. N. J. Persson, *Phys. Rev. B* **34**, 8941 (1986).

²⁷B. E. Hayden, K. Prince, D. P. Woodruff, and A. M. Bradshaw, *Phys. Rev. Lett.* **51**, 475 (1983).

²⁸C. Noda and G. E. Ewing, *Surf. Sci.* **240**, 181 (1990).

²⁹J. Evans, B. Hayden, F. Mosselmans, and A. Murray, *Surf. Sci.* **301**, 61 (1994).

³⁰D. P. Woodruff, B. E. Hayden, K. Prince, and A. M. Bradshaw, *Surf. Sci.* **123**, 397 (1982).

³¹R. Disselkamp, H.-C. Chang, and G. E. Ewing, *Surf. Sci.* **240**, 193 (1990).